Electronic Supplementary Information

Introduction of electron-deficient unit in resorcinol-formaldehyde resin to construct donor-acceptor conjugated polymer for enhancing photocatalytic H$_2$O$_2$ production

Xinyue Li, Qiuang Zheng, Xiaoran Wang, Qiuyu Zheng, Yi Zhang, Yanqing Cong[*],

Shi-Wen Lv[*],

School of Environmental Science and Engineering, Zhejiang Gongshang University, Hangzhou 310018, China

_____

*Corresponding author.

Mail to: No.18 Xuezheng Road, Hangzhou, 310018, China.

Email: yqcong@zjgsu.edu.cn (Yanqing Cong)

lvshiwen@zjgsu.edu.cn (Shi-Wen Lv)

Measurement of apparent quantum efficiency

The measurement of apparent quantum efficiency (AQE) was similarly carried out according to literature. AQE was measured under the illumination of a 300 W Xe lamp with different bandpass of 400, 450, 500, 550 and 600 nm. After ultrasonication and air bubbling, the photocatalytic reaction was carried out in pure deionized water (100 mL) with photocatalyst (10 mg). AQY was calculated by the following formula:

$$AQY = \frac{2 \times H_2O_2 \; formed \; (mol)}{the \; number \; of \; incident \; photons \; (mol)} \times 100\%$$

Measurement of solar-to-chemical energy conversion efficiency

According to the experimental method, the solar-to-chemical energy conversion (SCC) efficiency was determined by the photocatalytic experiments using an AM 1.5G spectrum as the light source (100 mW cm^{-2}). After air bubbling, the photocatalytic reaction was carried out in pure deionized water (100 mL) with photocatalyst (10 mg). The SCC efficiency was calculated via following equation:

$$SCC(\%) = \frac{\left[\Delta G \; for \; H_2O_2 \; generation \; (J \; mol^{-1})\right]\left[H_2O_2 \; formed \; (mol)\right]}{\left[total \; input \; power \; (W)\right]\left[reaction \; time \; (s)\right]} \times 100\%$$

where $\Delta G = 117$ kJ mol^{-1}. the energy intensity of the AM 1.5G solar irradiation (100 mW cm^{-2}), when using RF-BZ as the catalyst, the irradiated sample area was 4.5×5.2 cm^{-2}, so the total input power is 23.4 W.

Calculation method

Our spin-polarized density functional theory (DFT) calculations[1,2] were carried out in the Vienna ab initio simulation package (VASP) based on the plane-wave basis sets with the projector augmented-wave method[3,4]. The exchange-correlation potential was treated by using a generalized gradient approximation (GGA) with the Perdew-Burke-Ernzerhof (PBE) parametrization[5]. The van der Waals correction of Grimme's DFT-D3 model was also adopted[6]. The energy cutoff was set to be 500 eV. The Brillouin-zone integration was sampled with a Γ-centered Monkhorst-Pack mesh[7] of $1 \times 1 \times 1$. The structures were fully relaxed until the maximum force on each atom was less than 0.03 eV/Å, and the energy convergent standard was 10^{-5} eV. The adsorption energy E_{ads} per O_2 molecule can be defined as, $E_{ads} = E_{total} - E_{slab} - E_{mol}$, where E_{total} stands for the energy of the monolayer with the adsorbed O_2 molecule, E_{slab} is the energy of a clear monolayer, and E_{mol} is the energy of an O_2 molecule under vacuum.

References

1   Hohenberg, P. & Kohn, W. Inhomogeneous Electron Gas. *Physical Review* **136**, B864-B871, doi:10.1103/PhysRev.136.B864 (1964).

2   Kohn, W. & Sham, L. J. Self-Consistent Equations Including Exchange and Correlation Effects. *Physical Review* **140**, A1133-A1138, doi:10.1103/PhysRev.140.A1133 (1965).

3   Kresse, G. & Furthmüller, J. Efficient iterative schemes for ab initio total-energy calculations using a plane-wave basis set. *Physical review B* **54**, 11169 (1996).

4   Blöchl, P. E. Projector augmented-wave method. *Physical Review B* **50**, 17953-17979, doi:10.1103/PhysRevB.50.17953 (1994).

5   Perdew, J. P., Burke, K. & Ernzerhof, M. Generalized gradient approximation made simple. *Physical review letters* **77**, 3865 (1996).

6   Grimme, S., Antony, J., Ehrlich, S. & Krieg, H. A consistent and accurate ab initio parametrization of density functional dispersion correction (DFT-D) for the 94 elements H-Pu. *J Chem Phys* **132**, 154104, doi:10.1063/1.3382344 (2010).

7   Monkhorst, H. J. & Pack, J. D. Special points for Brillouin-zone integrations. *Physical Review B* **13**, 5188-5192, doi:10.1103/PhysRevB.13.5188 (1976).
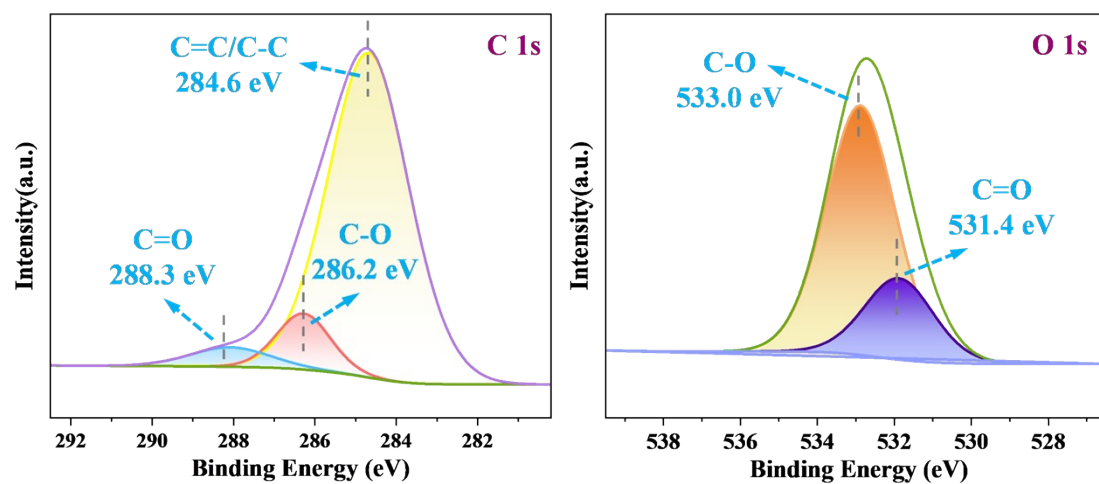
Content

Fig. S1. The high-resolution XPS spectra of RF: C 1s and O 1s.

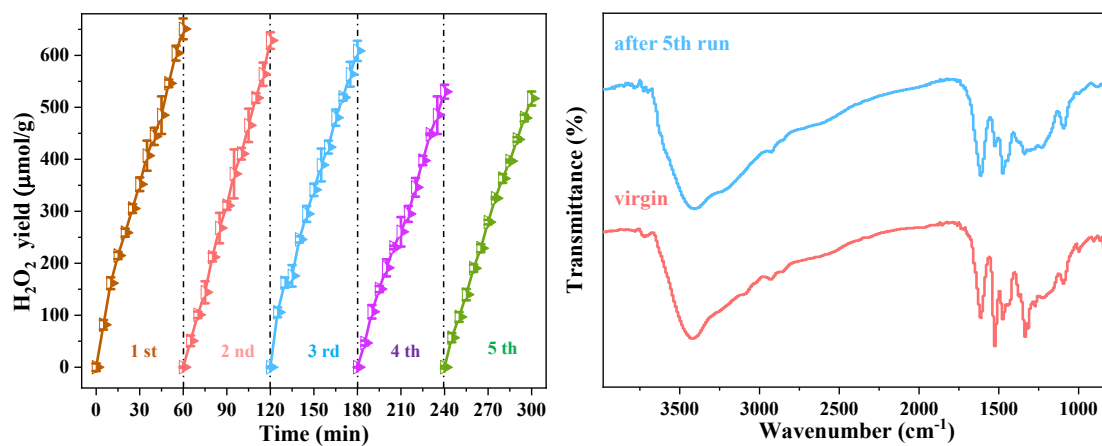**Fig. S2.** The cycling runs for photocatalytic H_2O_2 evolution over RF-BZ (left). The FT-IR spectra of RF-BZ after completing reaction (right).
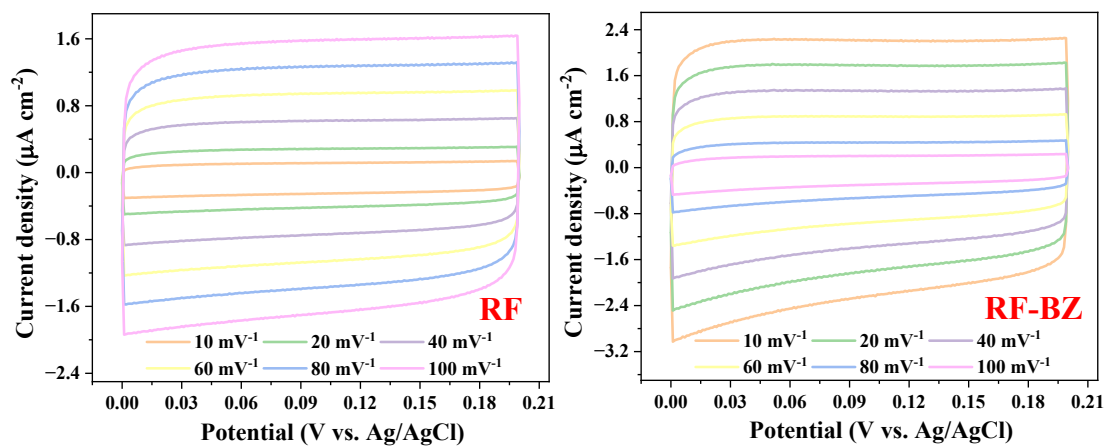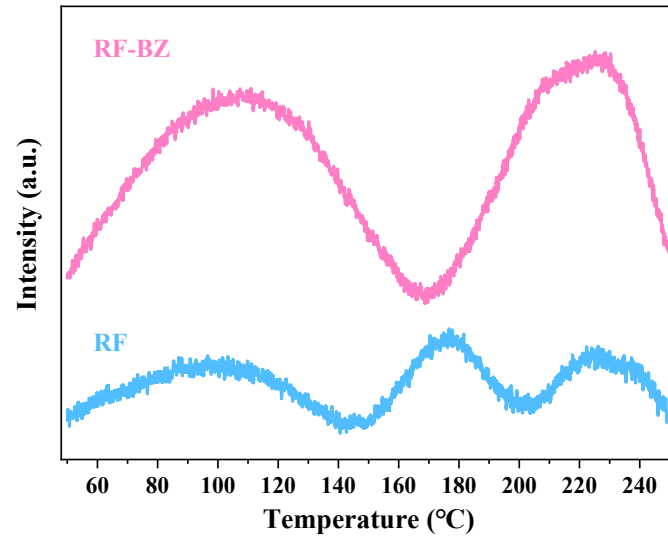
Fig. S3. CV curves of samples.

Fig. S4. The O_2 adsorption spectra of samples.

Fig. S5. The extinction coefficients of samples.

Fig. S6. Time courses of H_2O_2 production over RF-BZ under light irradiation.

Fig. S7. Effects of pH values on photocatalytic H_2O_2 generation.

Fig. S8. Tauc's band-gap plots of RF.

Fig. S9. Mott-Schottky plots of RF and RF-BZ.

Table S1. The wavelength-dependent AQY for photocatalytic H_2O_2 generation.

Fig. S1. The high-resolution XPS spectra of RF: C 1s and O 1s.

Fig. S2. The cycling runs for photocatalytic H_2O_2 evolution over RF-BZ (left). The FT-IR spectra of RF-BZ after completing reaction (right).

Fig. S3. CV curves of samples.

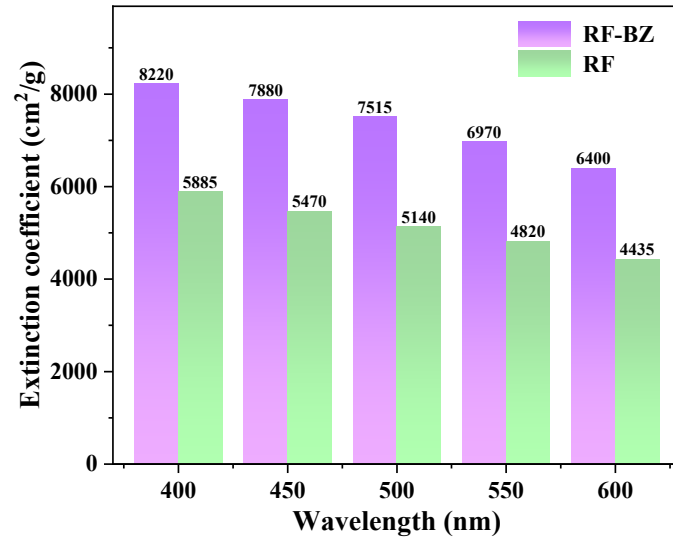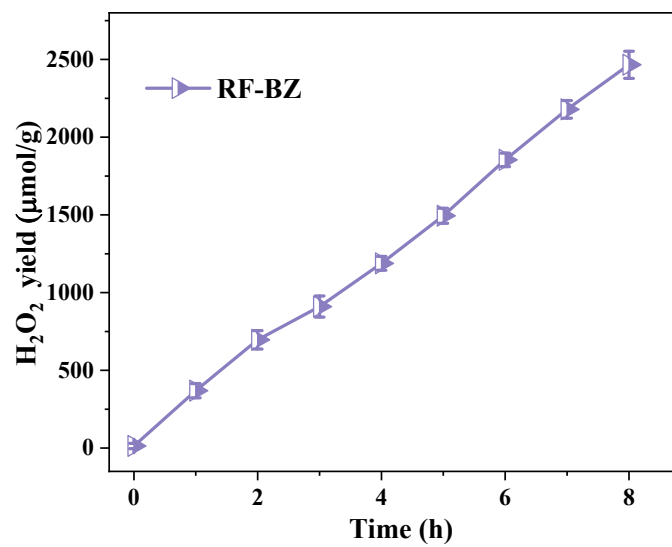**Fig. S4.** The O_2 adsorption spectra of samples.

Fig. S5. The extinction coefficients of samples.

Fig. S6. Time courses of H_2O_2 production over RF-BZ under light irradiation.
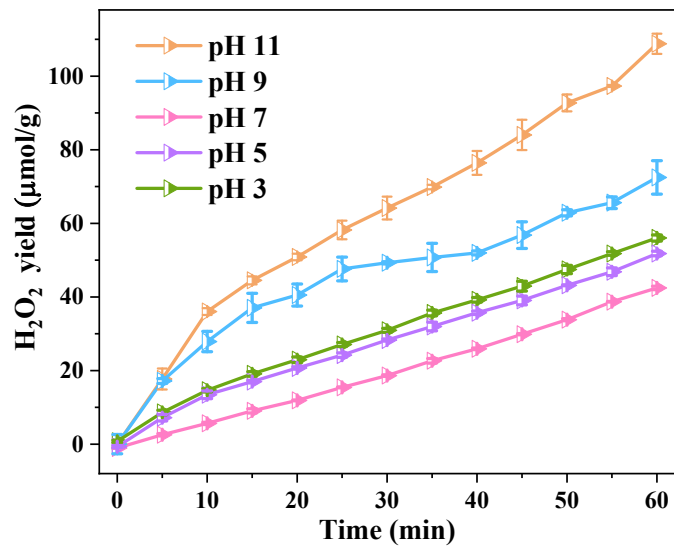
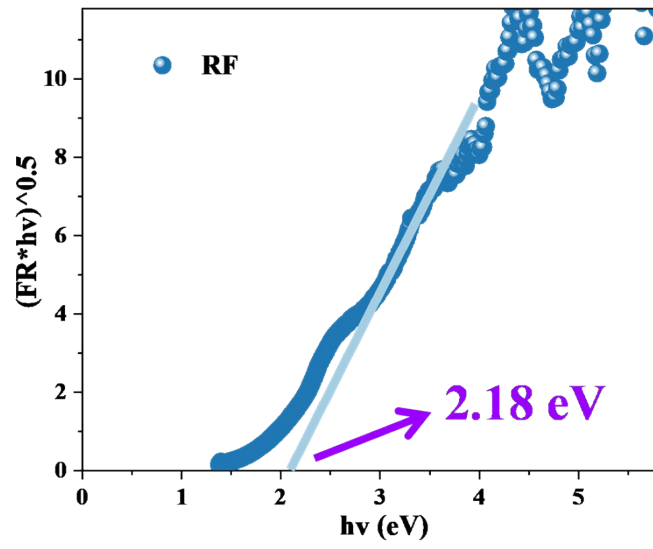**Fig. S7.** Effects of pH values on photocatalytic H_2O_2 generation.

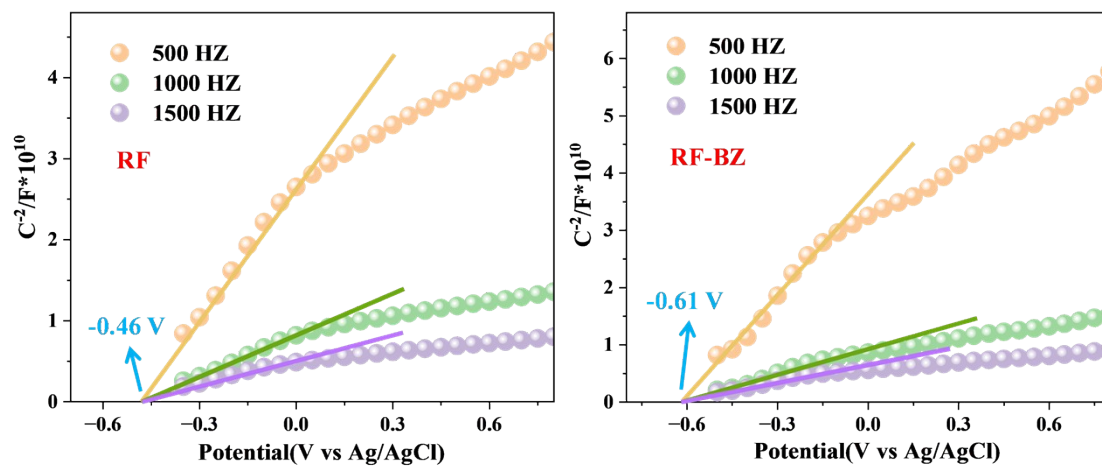**Fig. S8.** Tauc's band-gap plots of RF.

Fig. S9. Mott-Schottky plots of RF and RF-BZ.

Table S1. The wavelength-dependent AQY for photocatalytic H_2O_2 generation.

Wavelength (nm)	Light intensity (mW cm^{-2})	H_2O_2 evolution (umol)	Irradiation time (h)	AQY(%)
400	6.6	16.05842	1	40.43855
450	11.6	23.89347	1	30.43024
500	7.55	10.73196	1	18.89987
550	27.2	21.24742	1	9.44216
600	51	12.00344	1	2.607839